physica status solidi pss
www.pss-a.com

Interaction Between Hydrogen and Vacancy Defects in Crystalline Silicon

Ilia L. Kolevatov, Philip M. Weiser, Eduard V. Monakhov, and Bengt G. Svensson*

Hydrogen is one of the most important impurities in silicon. It is a mobile and highly reactive species that can passivate dangling bonds at dislocations, surfaces, and interfaces, which has been widely used in the microelectronics and solar cell industry for improving device performance. Vacancy defects are elementary complexes containing dangling bonds, and the study of their interaction with hydrogen is of significant importance. In this work, the interactions of hydrogen with the vacancy-oxygen complex (VO) and the divacancy (V_2) are discussed, which are the most dominant and fundamental vacancy defects stable at room temperature. It is shown that VO and V_2 can interact with both atomic and diatomic hydrogen species. This complicates the interpretation of experimental data and results in different reaction paths in differently prepared samples. Besides, some of important electronic properties, particularly electronic levels for V_2H_n with $n > 1$, are not experimentally established.

1. Introduction

It has long been realized that hydrogen (H) is one of the most important impurities in semiconductors (see ref. [1] and references therein). Hydrogen in Si is a mobile and highly-reactive species even at room temperature and saturates dangling bonds at the crystal surface,[2] at dislocations,[3] and at the interface between silicon and silicon oxide.[4] This property has been widely used in the microelectronics and solar cell industry for improving device performance.[5,6] In addition, recently there has been a renewed interest in H due to contradictory reports that H both suppresses and enhances light-induced degradation.[6–10] Vacancy-related defects are fundamental complexes containing dangling bonds. Therefore, the study of hydrogen-vacancy interactions is expected to be an important topic for years to come.

Vacancies (V) are highly mobile defects in Si and migrate at temperatures between 70 and 200 K, forming complexes with other defects and impurities.[11] Interstitial oxygen (O_i) is the most abundant impurity in Czochralski-grown silicon (Cz-Si) with concentrations in as-grown wafers of $\approx 10^{18}\,cm^{-3}$. Even in float-zone grown silicon (Fz-Si), the O_i concentration can be as high as $10^{16}\,cm^{-3}$. Hence, O_i is the dominant sink for migrating vacancies, forming the vacancy-oxygen center (VO), that is, the A-center. Another vacancy-defect, the divacancy (V_2), forms by self-trapping of vacancies. Thus, V_2 and VO are dominant vacancy-related complexes stable at room temperature.

In the present work, we will review the recent theoretical and experimental results on hydrogen and its interaction with vacancy-related complexes, focusing on the most prominent vacancy-complexes, VO, and V_2.

Dr. I. L. Kolevatov, Dr. P. M. Weiser, Prof. E. V. Monakhov, Prof. B. G. Svensson
Department of Physics
University of Oslo
Center for Materials Science and Nanotechnology
P.O.Box 1048 Blindern, N-0316 Oslo, Norway
E-mail: ilia.kolevatov@fys.uio.no

DOI: 10.1002/pssa.201800670

2. Atomic and Diatomic Hydrogen in Silicon

2.1. Atomic Hydrogen

Hydrogen in Si can be present in both atomic and diatomic forms. **Figure 1** shows the calculated formation energy of the different forms of atomic and diatomic hydrogen in Si plotted as a function of Fermi level position in the band gap.[12] Atomic H is an interstitial defect (H_i) that exhibits an amphoteric, negative-U behavior, and is present in a charge state that counters the conductivity type. In n-type Si, H_i behaves normally as an acceptor and becomes negatively charged (H_i^-), occupying tetrahedral (T) sites. In p-type Si, H_i is a donor and becomes positively charged (H_i^+), occupying bond-centered sites (BC).[12–14] As seen from Figure 1 the neutral charge state H_i^0 is always metastable compared to the charged states. The charge state transition level for the donor state, denoted $H_i(0/+)$, is higher in band gap than the charge state transition level for the acceptor state, denoted $H_i(-/0)$.[12,13,15] Deep-level transient spectroscopy (DLTS) measurements have determined the position of $H_i(0/+)$ to be $\approx E_c - 0.175\,eV$[16,17] (E_c being the conduction band minimum), whereas the position of $H_i(-/0)$ is at $\approx E_c - 0.65$ eV.[18,19] The charge state transition levels calculated using density functional theory (DFT)[20,21] are consistent with the experimentally determined levels mentioned above. Electron paramagnetic resonance (EPR) and infrared (IR) absorption signatures of H_i were also identified.[22,23]

The negative-U behavior of H_i implies that, under thermal equilibrium, the fraction of H_i present as H_i^0 will be small

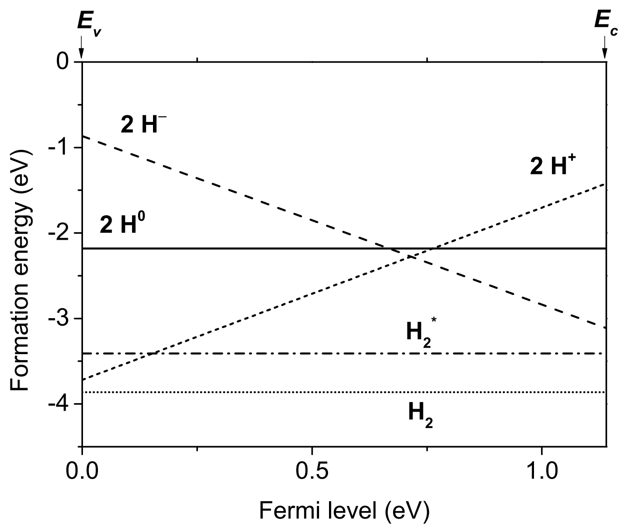

Figure 1. Formation energies for stable configurations of H in Si as a function of Fermi level position in band gap, based on data from ref. [12].

Bengt Gunnar Svensson completed a Ph.D. at CTH and GU in Gothenburg, Sweden (1980). Bengt became an Associate Professor (1987) and then a Professor (1997) at KTH, Sweden. He became a Professor at University of Oslo (2000) and founded a Semiconductor Physics group which grew from ≈10 to ≈50 people under his leadership. Bengt made significant contributions to the studies of defects, doping and diffusion in Si, SiC, SiGe; functional oxides, etc. He was a member of both IEEE and MRS, and was also an APS Fellow since 2014. Bengt passed away in July 2018 while the present work was being prepared for publication. He was not only an outstanding scientist but also an incredible mentor for many generations of physicists.

compared to H_i^+ (H_i^-) in p- (n-) type Si. As a result, experimental studies on the properties of H_i^0 are quite scarce. The neutral charge state H_i^0 can be found at both *BC* and *T* sites. The energy barrier for the $H_{BC}^0 \rightarrow H_T^0$ transition has been experimentally estimated to be ≈0.3 eV, while the energy barrier for the reverse transition ($H_T \rightarrow H_{BC}^0$) has been measured to be ≈0.2 eV.[17,19] There is a reason to believe that increasing the fraction of H_i^0 could have substantial benefits. As noted in ref. [24], H_i^0 has a diffusivity that is substantially higher than those of H_i^+ and H_i^-, making it the preferable diffusing species to passivate dangling bonds. Hamer et al.[25] reported that the effective minority carrier lifetime in p-type wafers was improved by up to a factor of ≈3 for wafers annealed between 400 and 700 K under illumination by a 90 W, 660-nm LED as compared to wafers annealed in the dark, presumably due to the increase in the fraction of H_i^0 generated by the illumination. Indeed, the activation energy of the H_i^0 diffusion has been estimated to be less than 0.1 eV[17,19] while the diffusion energy of H_i^+ has been measured to be in the range of 0.43–0.48 eV in a wide range of temperatures.[17,26,27]

Hydrogen atoms prefer to occupy *T* or *BC* sites in the vicinity of O_i which perturbs the crystal lattice and provides a more spacious environment for H_i. The resulted weakly-bound oxygen-hydrogen complex (O_i–H) exhibits properties similar to those of free H_i in Si giving rise to acceptor and donor states in band gap at $\approx E_c - 0.68$ eV and $\approx E_c - 0.175$ eV, respectively.[17,19] Similar to the isolated H_i, the O_i–H complex is also a negative-*U* center.

2.2. Diatomic Hydrogen

Diatomic hydrogen is present in the form of two different species: the isolated hydrogen molecule (H_2) and the hydrogen dimer (H_2^*). In free space, hydrogen molecules are both infrared and electrically inactive, which restricts their characterization typically to Raman spectroscopy. However, it was recognized that the crystal field of the host lattice could perturb the symmetry of the trapped H_2 molecules, permitting weakly allowed IR transitions. Consequently, both IR and Raman spectroscopies have been used to characterize H_2 in Si.[28–37] Since the beginning of the 1980s, theory has predicted that molecular H_2 should be energetically preferable than atomic H_i in Si.[38,39] As seen in Figure 1, the formation energy of H_2 is lower than that of two separated H_i, regardless of the charge state, for all Fermi-level positions within the band gap.

Early theoretical calculations were in agreement on the position of H_2 in the lattice at a *T* site. However, the early predictions on the activation energy for diffusion showed a considerable variation in the range of 0.6–2.7 eV.[14,38–40] Later, Markevich and Suezawa[31] experimentally determined the activation energy for H_2 diffusion to be 0.78 eV. This result was supported by calculations from Hourahine et al.[41] where the migration energy for H_2 was found to be 0.72 eV.

The barrier to the H_2 rotation was predicted to be relatively small, that is, H_2 should behave as a nearly-free rotator.[12,13,38–40,42] Chen et al.[35] have indeed shown that the thermally-activated behavior of the vibrational lines present in the IR absorbance spectra between 4.2 and 75 K for H_2, D_2, and HD molecules is consistent with the nearly-free rotator model for H_2 located at a *T* site proposed by theory. Subsequent uniaxial stress experiments[34,37] and theoretical modeling[43] confirmed the validity of this model. Hydrogen molecules have also been detected in Si using Raman spectroscopy. Both Murakami et al.[28] and Fukata et al.[29] reported the appearance of a vibrational line at 4158 cm^{-1} in Fz-Si hydrogenated using H-plasma and assigned it to isolated H_2 at a *T* site. However, Leitch et al.[33] argued that the 4158 cm^{-1} line originates from H_2 molecules trapped within voids in the crystal created by Si–H platelets that are formed during the plasma treatment. In fact, they detected a weaker vibrational line at 3618.4 cm^{-1} due to isolated H_2 molecules that was observed previously in IR experiments.[30] Following the publication of refs. [34,35,37,43], Lavrov and Weber[36] observed the characteristic ortho-para splitting of the vibrational lines assigned to isolated H_2, providing additional support for the assignment.

Hydrogen molecules tend to be trapped by O_i in O-rich Si, similar to atomic H. The O_i-H_2 complex was studied by both Markevich et al.[31] and Pritchard et al.[30] This center is present in silicon containing a substantial concentration of oxygen, that is, Cz-Si, after hydrogenation in an H_2 ambient at 1200 °C and, at 4.2 K, gives rise to two oxygen-related vibrational lines at 1075 and 1076 cm^{-1} and a pair of hydrogen-related vibrational lines at 3789 and 3731 cm^{-1}. Following the discovery of the thermally activated vibrational lines for the isolated H_2 molecule, Chen et al.[44] extended their nearly-free rotator model to the O_i–H_2 defect and showed that the H-related lines are also consistent with a nearly free rotator model for H_2, whereas the two O-related lines at 1075 and 1076 cm^{-1} are due to interactions of O_i with ortho- (O_i-oH_2) and para-H_2 (O_i-pH_2) molecules. Markevich and Suezawa[31] determined the binding energy for the O_i-H_2 complex to be 0.28 eV. Annealing studies by Pritchard et al.[32] showed that O_i-H_2 undergoes a reversible conversion to H_2 at temperatures between 35 and 130 °C. Annealing at higher temperatures (130–320 °C) results in a decrease in the O_i-H_2 concentration and no change in the H_2 concentration, that is, there is another sink for hydrogen that is not detected in these experiments.[30] Moreover, the experiment revealed that almost all of the hydrogen introduced by annealing in H_2 atmosphere followed by quenching is present in the molecular form.[32]

Despite the energetic preference for H_2 molecules, ab initio calculations have shown that H_2 molecules are easily dissociated due to interactions with intrinsic defects. Estreicher et al.[45] showed that silicon vacancies (V) and self-interstitials (I) readily dissociate H_2, which results in a net gain in potential energy of 4.0 and 1.7 eV, respectively. The dissociation is driven by the lattice strain created by intrinsic defects and is an important consideration for non-equilibrium processes, for example, etching, contact deposition, rapid thermal annealing, etc.[45]

An alternative type of diatomic hydrogen, $H_2{}^*$, was predicted theoretically[14,46] and, later, observed experimentally.[47] This complex consists of two separate H atoms located at neighboring *BC* and antibonding (*AB*) sites of silicon lattice. Both H atoms are bonded to neighboring Si atoms forming two Si—H bonds instead of H—H bond.[46] The total energy of this configuration is expected to be lower than that of two H_i[46] but higher than that of H_2 molecules.[40,46,48] The experimental observation of $H_2{}^*$ was done by IR absorption studies of H-implanted silicon.[47] The isotopic shift in combination with uniaxial stress experiments indicated that four observed Si—H modes originate from a trigonal defect involving two H atoms. Ab initio calculations confirmed that the observed IR bands are related to the dimer $H_2{}^*$.[47]

2.3. Hydrogen Introduction into Silicon

Hydrogen can easily penetrate into Si. The standard chemical treatment of Si wafers using hydrofluoric acid (HF) enriches several microns below the surface with H at room temperature.[5] Hydrogen can be incorporated into Si even by immersion of wafers into boiling water.[49] Hydrogenation of Si can be performed using several different approaches that vary with the amount of H incorporated into the material and the amount of surface and lattice damage.

Ion implantation is one of the possible techniques. Hydrogen or deuterium (D) ions are accelerated by an electric field and penetrate into silicon substrate. This implantation process is inevitably accompanied by the creation of irradiation-induced defects such as, for example, V and I. The ion penetration depth into the substrate is controlled by the energy of the ions whereas the amount of H incorporated into that region is determined by the implantation dose. The available energy range depends on the construction of implanter. For example, a tandem accelerator operates at energies ≈10 keV–10 MeV[50] and is suitable for hydrogenation of Si wafers throughout the bulk, whereas a Kaufman source[5,51,52] implants ions in a near surface region with energies typically below 1 keV.

Hydrogen plasma treatment can also be used for the hydrogenation of the silicon wafers.[53] This method occurs at elevated temperature (≈150–300 °C). For example, plasma hydrogenation at 300 °C for 2 h can result in a H concentration of $\approx 10^{20}$ cm^{-3} near the exposed surface.[53] However, plasma treatments also create a substantial amount of damage to the exposed surface that may or may not be beneficial for the material. The surface damage can be reduced by placing the material further away from the plasma or reducing the kinetic energy of the ion before it reaches the material.[5]

The deposition of various Si_xN_y antireflection coatings by plasma-enhanced chemical vapor deposition (PECVD) on Si solar cells can also incorporate significant amounts of hydrogen. The PECVD process of Si_xN_y deposition involves H-containing gases, and the deposited film has a high H-concentration.[54] The total amount of H was inferred as ≈20% in the film deposited at 350 °C from SiH_4/NH_3 gases.[54] The following processing normally takes place at elevated temperatures, which introduces H into the bulk of Si.[8,9]

Hydrogen can be incorporated by annealing at 1000–1300 °C in H_2 ambient followed by quenching. This treatment ensures that the majority of H is present in a diatomic form.[55] The vibrational modes of H_2 molecules in the vicinity of O_i, as well as a mode for $H_2{}^*$, were observed in such a material.[56]

3. Vacancy-Oxygen and Hydrogen

Silicon wafers have normally a high concentration of oxygen ($\approx 10^{16}$–10^{18} cm^{-3} for Fz-Si and Cz-Si) making it a dominant sink for V.[60] Given the above discussion on the presence of hydrogen, it is not surprising that hydrogen also interacts with vacancy-oxygen complexes (VO) to form additional defects. **Figure 2** shows the structure of VO as well as the structures of the primary vacancy-oxygen-hydrogen defects VOH and VOH$_2$.

The vacancy-oxygen complex is one of the longest-recognized defects in Si, being studied first by EPR and electrical measurements in 1959[61,62] and later by IR spectroscopy.[57] The vacancy defect in Si gives rise to four dangling bonds: O_i binds to two of them, and the remaining two dangling bonds form an elongated covalent bond that is responsible for the electronic activity of VO. Both EPR and electrical measurements[61,62] concluded that VO can act as an acceptor, existing in either the negative (VO$^-$) or neutral (VO^0) charge states with a charge-state transition VO(−/0) level at $E_c-0.17$ eV. This position is close to the position $E_c-0.13$ eV determined by theory.[21] The two different charge states of the VO center give

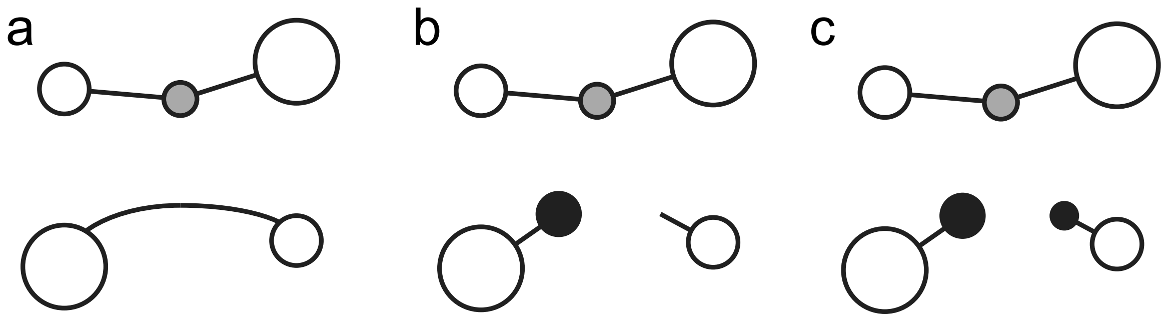

Figure 2. The atomic structures for (a) *VO*, (b) *VOH*, (c) *VOH*$_2$ viewed along <100>, based on refs. [56–59]. White, black, and gray atoms are Si, H, and O, respectively. The larger atoms are closer to the reader.

rise to different localized vibrational modes (LVMs) in the IR absorbance spectrum due to the difference in the amount of charge localized in the bonds. Both charge states, VO^0 and VO^-, give rise to three vibrational modes (see **Table 1**),[57,63] which are associated with the Si–O–Si pseudomolecule. The different wavenumbers of these vibrations compared to those of the isolated O_i is a reflection of the additional volume available to the oxygen atom due to the presence of *V*. The $\approx$50 cm^{-1} increase in the vibrational frequency for VO^- compared to VO^0 is due to the repulsion between the extra electron localized on the reconstructed Si—Si bond and the negatively polarized O atom.[59] Uniaxial stress experiments were performed to determine the point group symmetry and associated thermodynamic properties, that is, the activation energy for reorientation, using both EPR and IR spectroscopies.[57,64] From these experiments, *VO* was found to have C_{2v} symmetry (consistent with the picture

Table 1. Electrical and infrared absorption characteristics of complexes discussed in present work.

Complex	Electronic level [eV] and charge state	Capture cross-section for major charge carriers [cm^2]	Wave number [cm^{-1}] and temperature of measurement	Notes and references
H_i	E_c – 0.175 (0/+) E_c – 0.65 (–/0)	No detailed information	1998 at 9 K (H_{BC}^+)	DLTS: refs. [16,18,19] IR: ref. [23]
O_i-H	E_c – 0.175 (0/+) E_c – 0.68 (–/0)	No detailed information	No detailed information	DLTS: refs. [17,19]
H_2	Neutral	Neutral	3618.4 (Q(0)) at 10 K	IR: ref. [32]
O_i-H_2	Neutral	Neutral	1075.1(O_i-pH_2) 1076.6 (O_i–oH_2) 3731.0 (oH_2, Q(1)) 3737.1 (oH_2, Q(0)) 3788.9 (pH_2, Q(1))	IR: refs. [30,44]
H_2^*	Neutral	Neutral	817.2; 1599.1; 1838.3; 2061.5 at 77 K	IR: ref. [47]
V_2	E_c – 0.23 (=/–) E_c – 0.42 (–/0) E_v + 0.19 (0/+)	10^{-15} 2×10^{-15} 10^{-16}	5880 V_2^0 3020; 2890; 2767 V_2– 2560 V_2^+ at 4.2 K	DLTS: refs. [71,82,83] IR ref. [84] *Electronic IR absorption only
V_2H	$\approx E_c$ – 0.43 (–/0)	Unknown	2068.1 at 12 K	L-DLTS: ref. [69] IR: ref. [78]
V_2H_2	E_c – 0.32 (–/0) (theory)	Unknown	2072 at 7 K	DFT: ref. [79] IR: ref. [94]
V_2H_6	Neutral	Neutral	2166; 2191 at 10 K	IR: refs. [23,95]
VO	E_c – 0.17 (–/0)	10^{-14}	1430.1; 885.2; $\approx$545 VO^- 1370; 835.8; $\approx$534 VO^0 at 10 K	DLTS: refs. [82,83] IR: refs. [57,63]
VOH	E_c – 0.32 (–/0) E_v + 0.27 (0/+)	3×10^{-15} 10^{-14}	870 at 80 K (exp.) 2042.4; 854.4; 578.5; 565.2; 532.5 (theory)	DLTS: refs. [71,83] IR: ref. DFT: ref. [59]
VOH*	E_c – 0.37	8×10^{-15}	Unknown	DLTS ref. [98]
VOH$_2$	Neutral	Neutral	943.5; 2126.4; 2151.5 At 10 K	IR refs. [56,76]

of an Si–O–Si pseudomolecule) and an activation energy for reorientation of ≈0.4 eV for the oxygen to jump between the different Si—Si bonds.[57,64]

The *V*O center anneals out at temperatures above 300 °C to form the VO_2 complex.[65–68] This conversion has been shown to take place mainly via the diffusion of *V*O and subsequent trapping by O_i.[67] On one hand, this reaction is consistent with the dependence of the annealing rate on the O_i concentration. On the other hand, *V*O and VO_2 do not follow a one-to-one proportionality, which suggests another reaction contributes to the annealing kinetics.[65] The dissociation of *V*O, $VO \rightarrow V + O_i$, is a strong candidate for this reaction.[65] Although the released *V*'s are recaptured mainly by O_i, they can also be trapped by other radiation-induced interstitial defects.[67] Based on the findings of several studies,[65–68] the activation energies for dissociation and diffusion of *V*O are ≈2.5 and 1.7 eV, respectively.

Both atomic and molecular H diffuse at temperatures significantly lower than 300 °C making reactions with hydrogen dominant for the annealing of *V*O in hydrogen-containing Si. The interaction of *V*O with one H-atom results in a formation of vacancy-oxygen-hydrogen (*V*OH) complexes. The atomic structure of *V*OH is shown in Figure 2. The H atom breaks the reconstructed Si—Si bond and forms a Si—H bond with only one of the Si atoms. The remaining dangling bond of the second Si atom is responsible for the electrical activity of the *V*OH center. The vacancy-oxygen-hydrogen complex can be found in all three charge states: negative (−), positive (+), or neutral (0). This defect has an acceptor (−/0) level in the upper part of the band gap at $E_c-0.32$ eV and a donor (+/0) level in the lower part of the band gap at $E_v+0.27$ eV (E_v being the valence band maximum).[69–71] These levels are observed together by DLTS and minority-carrier transient spectroscopy (MCTS) after H-implantation[70,71] as well as after H-diffusion from acid solution into electron-irradiated n-type silicon.[72,73] **Figure 3**a shows the amplitudes of the signals from *V*OH−/0), *V*OH(0/+), and *V*O(−/0) deduced from DLTS and MCTS measurements as a function of annealing temperature. Upon annealing at 100 °C and above, the amplitude of the *V*O(−/0) signal decreases and the amplitudes of the *V*OH signals increase, providing evidence for the reaction $VO + H \rightarrow VOH$. Figure 3b shows that the two signals attributed to *V*OH have nearly equal amplitudes regardless of the growth or doping of the Si wafer, providing strong evidence for their assignment to two charge state transition-levels of the same defect.[70]

The symmetry of *V*OH has been determined from EPR measurements of VOH^0 in H- and D-implanted Cz-Si samples subjected to uniaxial stress.[58] At temperatures below 240 K, the defect is static and shows C_{1h} symmetry. However, at temperatures above 240 K, the splitting of the EPR signal changes and coincides with a defect with C_{2v} symmetry. The change in the symmetry of the defect at 240 K has been explained in terms of a dynamical reorientation of the hydrogen atom. That is, H jumps between the two equivalent dangling bonds of the Si atoms (not bonded with O). The activation energy for reorientation was found to be 0.18 eV for H and 0.26 eV for D, which is quite surprising given that the energy needed to break a Si—H bond is estimated to be ≈3.3 eV.[74] The results of Laplace-DLTS (L-DLTS) study combined with uniaxial stress[69] are consistent with the defect symmetry determined by EPR.

Ab initio calculations[59] predict that the *V*OH defect should give rise to LVMs at 2042.4, 854.5, 578.5, 565.2, and 532.5 cm^{-1}. Aside from the attribution by Mukashev et al.[75] of an IR-absorption line located at 870 cm^{-1} at 80 K to the Si–O–Si stretching mode of the *V*OH defect, no H-related LVMs have been detected.

Hydrogen can also passivate the second dangling bond in the *V*OH complex resulting in a vacancy-oxygen complex containing two hydrogen atoms (VOH_2). DFT has predicted that the arrangement of the defect with the two H atoms placed inside the vacancy, that is, the Si—H bonds point into the vacancy, is energetically preferable by ≈1.25 eV over the structure with the H atoms outside the vacancy.[56,76] The complex is electrically inactive because both of the Si dangling bonds are passivated with H. Markevich et al.[56] observed the formation of VOH_2 using IR spectroscopy for Cz-Si samples that were hydrogenated in an H_2 ambient (1200 °C for 1 h followed by quenching) and subsequently irradiated with 3 MeV electrons near 50 °C. The hydrogenation and quenching produces a reservoir of hydrogen mainly in the form of O_i–H_2 and H_2^* complexes. The subsequent electron irradiation provides a large source of

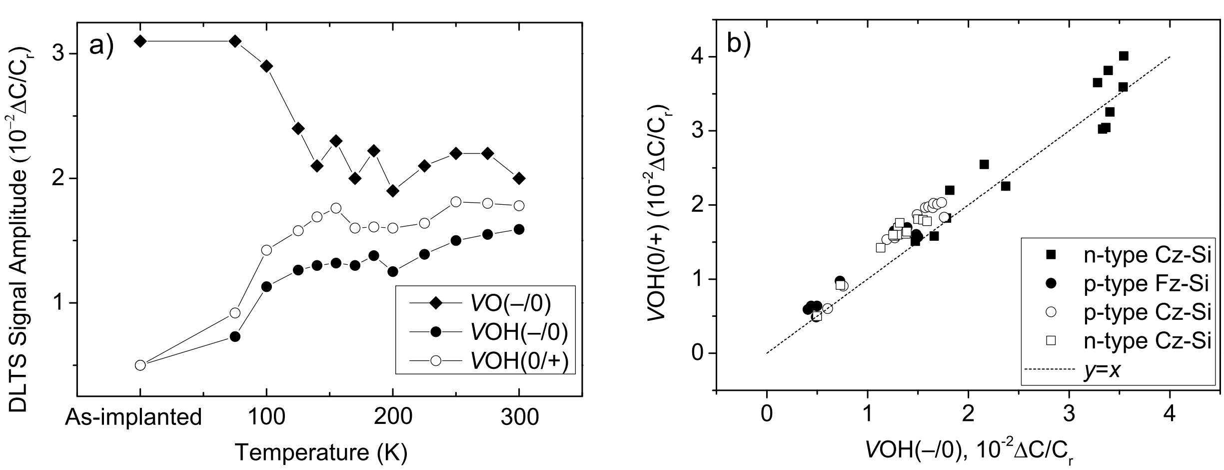

Figure 3. a) The DLTS/MCTS amplitudes of *V*O(−/0), *V*OH(−/0), and *V*OH(0/+) in an H-implanted Si sample at different stages of isochronal annealing. b) Correlation between the amplitudes of *V*OH(0/+) and *V*OH(−/0) in Cz-Si and Fz-Si samples. Data taken from ref. [70].

irradiation-induced defects, including VO and V_2. Annealing at 100 °C results in the decrease in the intensity of the IR lines due to these defects and the appearance of new IR lines at 943.5, 2126.4, and 2151.5 cm^{-1} at 10 K. The involvement of hydrogen was confirmed from the characteristic hydrogen/deuterium isotope shifts of the two high frequency IR lines for samples that were deuterated instead of hydrogenated. These lines have been assigned to vibrations of the antisymmetric stretching of Si–O–Si, and the antisymmetric and symmetric stretches of the two Si—H bonds, respectively.[56] The sample treatment presented in ref. [56] (hydrogenation, irradiation, and annealing) illuminates one potential pathway for the formation of VOH_2 via the reaction, $VO + H_2 \rightarrow VOH_2$. This reaction is consistent with the earlier discussion regarding H_2 dissociation by imperfections in the crystal.[45]

Although there is a consensus on the most stable atomic configurations of VOH_n complexes shown in Figure 2, the existence of other configurations cannot be ruled out. Bleka et al.[73] observed, for example, that the annealing of VO in chemically-hydrogenated high-purity n-type Fz-Si gave rise to a DLTS peak, labeled $E1$, with a position at E_c−0.37 eV. The formation of $E1$ occurred after annealing at 225 °C for 20 min and demonstrated one-to-one negative correlation with VO. Based on this evidence, the $E1$ peak was attributed to an unstable configuration of the vacancy-oxygen-hydrogen center (VOH^*). Further annealing at higher temperatures or for longer durations (≈42 h) resulted in the partial recovery of VO and the formation of the $VOH(-/0)$ level at E_c−0.32 eV.

4. Divacancy and Hydrogen

The divacancy (V_2) is another fundamental and well-studied intrinsic defect in silicon. Experiments have found that the defect can exist in the positive (+), neutral (0), negative (−), and doubly negative (=) charge states.[77,80,81] EPR experiments performed by Watkins and Corbett[77] provided a wealth of information on the properties of V_2. The unrelaxed structure of V_2 consists of two nearest neighbor vacancies, resulting in six dangling bonds. This structure is unstable and undergoes Jahn-Teller (JT) distortion: four of the dangling bonds reconstruct in a manner similar to the reconstruction of Si dangling bonds in VO, and the two remaining dangling bonds are responsible for the electrical activity of V_2. The JT-distorted defect (shown in **Figure 4**a) possesses C_{2h} symmetry, and additional electronic degeneracy is available due to the different configurations of the reconstructed bonds.[77,80] Both the electronic and atomic reorientation of V_2 were studied by EPR experiments. The electronic reorientation occurs between 30 and 110 K with a thermal activation energy of 60 meV for both the $V_2{}^+$ and $V_2{}^-$ charge states and increases the symmetry of V_2 from C_{2h} to D_{3d}.[77] Uniaxial stress studies observed a stress-induced alignment, that is, an atomic reorientation of the defect, that occurs with a thermal activation energy of ≈1.3 eV. Since the stress-induced reorientation also corresponds to the diffusion of V_2 through the Si lattice, this activation energy is also the activation energy for diffusion. The V_2 charge state transition-levels are E_v + 0.19 eV for $V_2(0/+)$, E_c−0.42 eV for $V_2(-/0)$ and

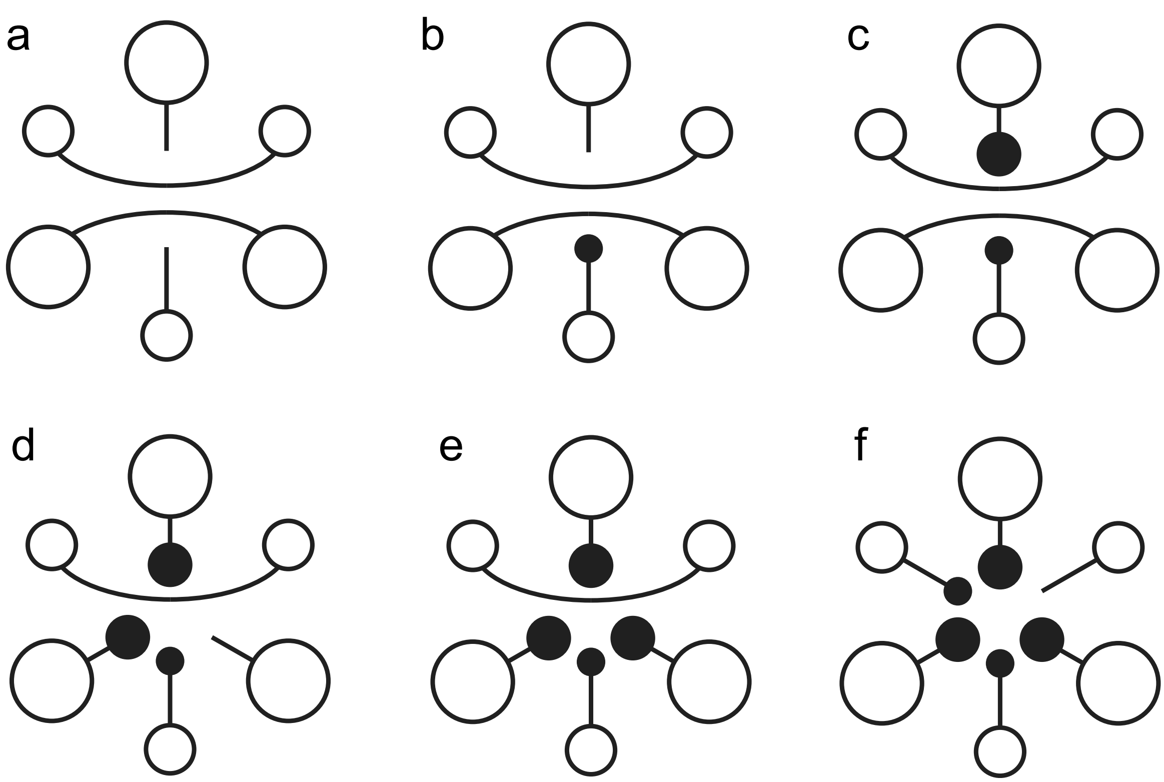

Figure 4. The atomic structures for(a) V_2, (b) V_2H, (c) V_2H_2, (d) V_2H_3, (e) V_2H_4, and (f) V_2H_5 viewed along the <111> crystalline axis, based on refs. [77–79]. White and black atoms are Si and H, respectively. The larger atoms are closer to the reader.

E_c−0.23 eV for $V_2(=/-)$.[71,82,83] Several electronic absorption features associated with V_2^+, V_2^0, and V_2^- have been identified in the IR absorption spectrum for samples measured at 4.2 K (see Table 1).[84]

Normally, a decrease in V_2 concentration occurs upon annealing at temperatures between 250 and 300 °C, and the resulting defect(s) depend on the background impurity content of the Si material. In the first studies, utilizing EPR, diffusion and dissociation were considered as two competing mechanisms for V_2 annealing with activation energies of around 1.3 and 1.6 eV, respectively.[77] On one hand, the diffusion mechanism dominates in oxygen-rich Cz-Si where V_2 can be trapped by O_i and forms the divacancy-oxygen complex (V_2O). On the other hand, the dissociation mechanism prevails in O-lean Fz-Si.[77] Later, Lee and Corbett observed the formation of V_2O during annealing of V_2.[85] In contrast to V_2, the electronic properties of V_2O were not experimentally established until the early 2000s (see refs. [86–88] and references therein).

In a number of studies, however, annealing of Cz-Si containing V_2 did not result in the formation V_2O (see, e.g., ref. [89]). This discrepancy was attributed to the effect of hydrogen, where the reaction between V_2 and hydrogen dominates due to a high mobility of hydrogen species.[90] **Figure 5** shows the DLTS spectra for hydrogenated and non-hydrogenated Si and the defect evolution upon isothermal annealing in this material.[90] The hydrogen-free sample (Figure 5a) demonstrates the interaction of diffusing V_2 with O_i upon isochronal annealing, where both states of V_2 transform into the corresponding V_2O states with one-to-one proportionality, while the *V*O signal remained almost constant. In contrast, the signals from the V_2 states in the hydrogenated sample (Figure 5b) anneal out rapidly in the same temperature range and without the emergence of signals due to V_2O.

Figure 4 shows the family of divacancy-hydrogen complexes (V_2H_n) that form due to H-passivation of V_2. The divacancy can accommodate up to six H atoms. The first two hydrogen atoms will passivate the dangling bonds remaining after JT distortion of V_2. Additional H-atoms ($n > 2$) will break the reconstructed Si—Si bonds and saturate the resulting dangling bonds. Five of these defects ($n < 6$) are expected to be electrically active whereas the fully passivated defect, V_2H_6, is expected to be electrically inactive.

Stallinga et al. observed an EPR signal labelled $S1_a$ in n-type Fz-Si implanted with hydrogen and deuterium ions at cryogenic temperatures.[78] Their results indicated that $S1_a$ was related to an unpaired electron at a dangling bond in planar vacancy-related complex with one H atom. The $S1_a$ signal was identified as uncharged V_2H by the hydrogen hyperfine interaction analysis. Fourier-transform infrared spectroscopy (FT-IR) measurements of a similar batch of samples were performed in the same work.[78] The line at 2068.1 cm^{-1} had an isotopic shift to 1507.6 cm^{-1} with a factor of $\approx\sqrt{2}$ upon the replacement of hydrogen by deuterium, indicating a hydrogen-containing complex. The uniaxial stress IR-measurements indicated that the origin of this mode has the same symmetry as that of V_2H. Upon isochronal annealing, the $S1_a$ and the IR-absorption signal at 2068.1 cm^{-1} decayed simultaneously. This suggests that the line at 2068.1 cm^{-1} is a stretch mode of the V_2H complex (see **Figure 6**). The reorientation of the V_2H complex occurs above 310 K through H jumps.[78]

The electronic properties of the divacancy-hydrogen defect family (V_2H_n) have not been established conclusively. The positions of electrical levels have been estimated with DFT calculations using the *marker method*.[79] The acceptor states of well-studied *V*OH and *V*O were chosen as markers for the $(-/0)$ levels of V_2H and V_2H_2, respectively; the donor level of *V*OH was a reference for the $(0/+)$ states of V_2H and V_2H_2. Analysis of the electronic structure placed $V_2H(-/0)$ at E_c–0.44 eV while the hole trap $V_2H(0/+)$ was predicted to occur at $E_v + 0.18$ eV. The V_2H_2 center is expected to give rise to only acceptor state at E_c−0.32 eV.[79] Thus, the V_2H states have energy positions close to those of V_2, and a strong overlap between the corresponding peaks is expected in the experiment. In addition, $V_2H_2(-/0)$ can overlap with $VOH(-/0)$, which are both placed by theory at E_c−0.32 eV. This fact complicates an experimental identification of the V_2H_n states.

There are, however, experimental indications on the presence of $V_2H(-/0)$ overlapping with $V_2(-/0)$. It has been consistently observed by DLTS that the amplitude of the $V_2(-/0)$ peak is greater than that of $V_2(=/-)$ with almost a two-to-one ratio for H-

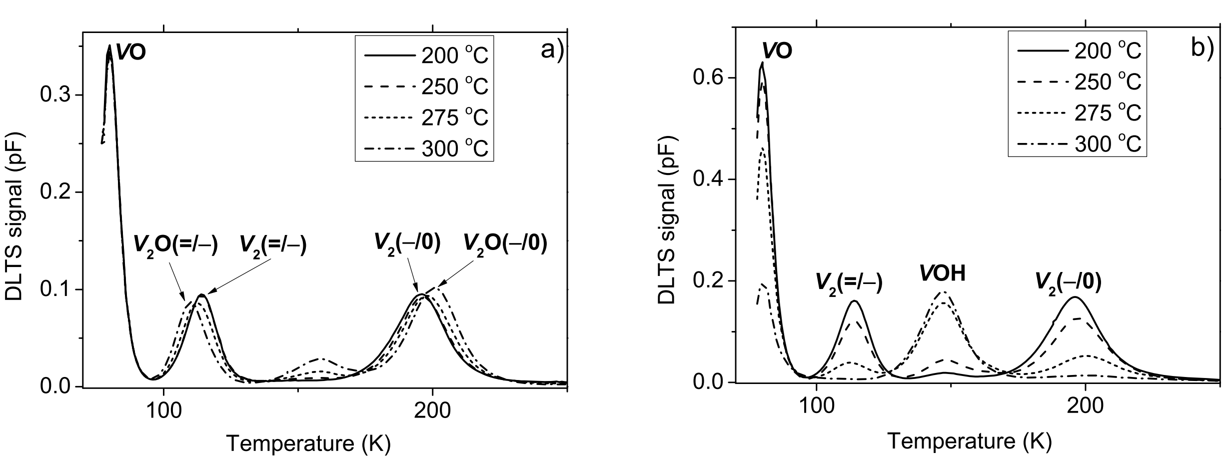

Figure 5. DLTS spectra of (a) hydrogen-free and (b) plasma-hydrogenated oxygen-enriched Fz-Si after different steps of isothermal annealing. Data are taken from ref. [90].

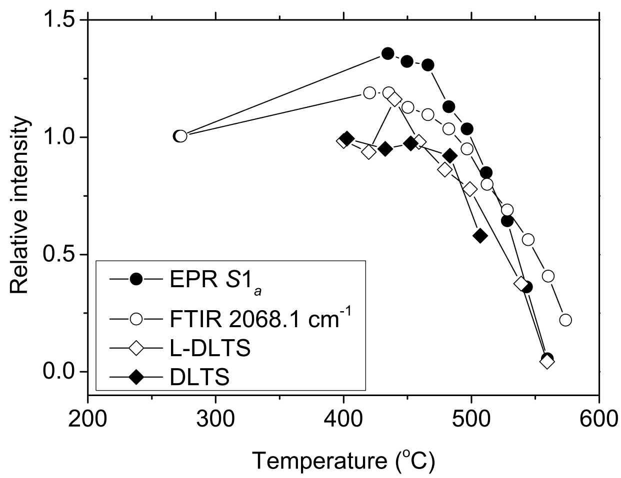

Figure 6. Relative intensities of the signals attributed to $V2$H by different measurement techniques (EPR,[78] FT-IR,[78] L-DLTS,[69] and DLTS[91]) as a function of the annealing temperature. Intensities were normalized with respect to their initial value.

implanted n-type Si, in contrast to hydrogen-free irradiated material where the $V_2(-/0)$ and $V_2(=/-)$ DLTS peaks show equal amplitudes.[69,70,73,91,92] Therefore, an additional H-related contribution in the DLTS peak of $V_2(-/0)$ was suggested. Typical DLTS spectra of H-implanted and H-free irradiated Cz-Si are shown in **Figure 7**, where the V_2 $(-/0)$ amplitude is larger than that of $V_2(=/-)$ indicating the V_2H$(-/0)$ contribution to the former state. This contribution demonstrated the decay kinetics similar to that of the EPR signal $S1_a$ mentioned above, and this state can be tentatively attributed to the V_2H complex.[69,91] Thus, the annealing of the EPR, IR, DLTS and L-DLTS signals occurs at the same temperature as shown in Figure 6.

There is, however, no indication of the V_2H$(-/0)$ level at E_c−0.44 eV, if H is introduced from hydrogen-plasma[90] or acid solution.[73] In these studies both DLTS peaks corresponding to $V_2(-/0)$ and $V_2(=/-)$ have the same amplitude even after annealing, which implies the absence of the V_2H$(-/0)$ level

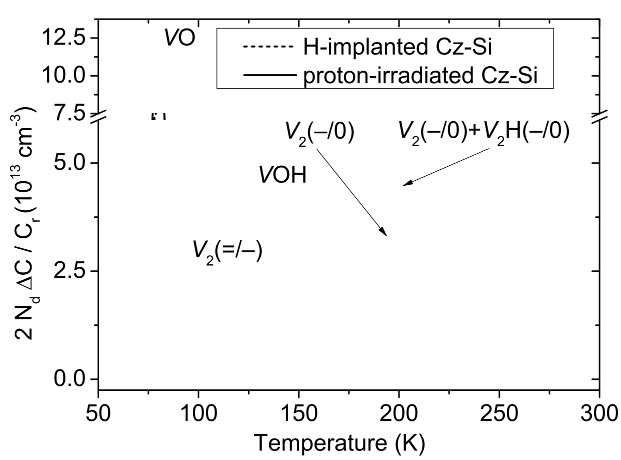

Figure 7. Deep level transient spectra of Cz-Si irradiated with protons to create only lattice damage (solid curve) or implanted with H (dashed curve). The data are taken from ref. [93].

overlapping with $V_2(-/0)$.[90] For instance, the DLTS spectra of H-plasma hydrogenated Si are presented in Figure 5b where both $V_2(=/-)$ and $V_2(-/0)$ peaks appear to have the same amplitudes after each step of isochronal annealing.

The absence of V_2H in these experiments can be explained if one assumes that the hydrogenation from acid solution or plasma results in H_2 or H_2^* as the dominant H species. In this case, the hydrogen-assisted annealing of V_2 can occur through the diffusion of H_2 or H_2^*, that is, the reactions $V_2 + H_2 \rightarrow V_2H_2$ or $V_2 + H_2^* \rightarrow V_2H_2$ can become dominant, and the formation of V_2H is not anticipated. However, no electronic level has been attributed conclusively to V_2H_2 until now. As mentioned above, the calculated energy position of V_2H_2 acceptor state predicts that the $V_2H_2(-/0)$ peak can overlap with the VOH$(-/0)$ peak, which complicates the experimental observation.[79]

An IR-band at 2072 cm^{-1} has been detected in Si hydrogenated from H_2 gas at 1300 °C and then electron-irradiated.[94] Such sample treatment incorporates hydrogen in the form of H_2.[32] This line was found to be proportional to the square root of electron dose and to contain two hydrogen atoms. This allowed attributing the 2072 cm^{-1} line to the vibration mode of the V_2H_2 center.[94] The V_2H_2 IR-band anneals out in the range of 150–300 °C.[94]

The formation of V_2H_n where $n = 3$–5 with a detectable concentration is challenging to implement experimentally. However, the IR-bands of V_2H_6 have been identified.[95,96] The IR-lines at 2166 and 2191 cm^{-1} were observed in H-implanted silicon and originated from a trigonal complex with at least three Si—H bonds.[96,97] The likely candidates were limited to the VH_3 and V_2H_6 centers with trigonal symmetry.[96] The vibrational modes of both complexes have been calculated to be very similar making their identification challenging.[23] However, the EPR signal of VH_3 was later identified and correlated with IR band at 2155 and 2182 cm^{-1}.[23] Thus, the lines at 2166 and 2191 cm^{-1} were attributed to the V_2H_6 complex.[23,95]

5. Conclusion

Although the atomic structures of such dominant complexes as VOH_m, $m = 0$, 1, 2; and V_2H_n, $n = 0$–6, appears to be widely accepted, some of their properties and formation kinetics are not experimentally established. It is now realized that VO and V_2 can interact with both atomic and diatomic hydrogen, resulting in different annealing kinetics in differently prepared samples. The existence of several hydrogen species (H_i, H_2, and H_2^*) complicate the interpretation of experimental data. Electronic properties of V_2H_n are also not confirmed experimentally. While there are good experimental evidences on the electronic levels for V_2H, the levels for V_2H_n with $n > 1$ are not experimentally identified.

Acknowledgments

This work was performed within "The Norwegian Research Centre for Solar Cell Technology" (project number 460976) and "The Research Center for Sustainable Solar Cell Technology" (project number 461418) cosponsored by the Norwegian Research Council and research and industry partners in Norway. The Research Council of Norway was acknowledged for the support to "The Norwegian Micro- and Nano-Fabrication Facility, NorFab" (project number 245963).

Conflict of Interest

The authors declare no conflict of interest.

Keywords

divacancy, hydrogen, silicon, vacancy defects, vacancy-oxygen

Received: August 23, 2018
Revised: October 8, 2018
Published online:

[1] C. G. Van de Walle, J. Neugebauer, *Annu. Rev. Mater. Res.* **2006**, *36*, 179.
[2] Y. J. Chabal, *Phys. B Condens. Matter* **1991**, *170*, 447.
[3] C. Dubé, J. I. Hanoka, *Appl. Phys. Lett.* **1984**, *45*, 1135.
[4] K. L. Brower, *Phys. Rev. B* **1988**, *38*, 9657.
[5] B. Sopori, Y. Zhang, N. M. Ravindra, *J. Electron. Mater.* **2001**, *30*, 1616.
[6] B. Hallam, A. Herguth, P. Hamer, N. Nampalli, S. Wilking, M. Abbott, S. Wenham, G. Hahn, *Appl. Sci.* **2017**, *8*, 10.
[7] G. Krugel, W. Wolke, J. Geilker, S. Rein, R. Preu, *Energy Procedia* **2011**, *8*, 47.
[8] S. Wilking, S. Ebert, A. Herguth, G. Hahn, *J. Appl. Phys.* **2013**, *114*, 194512.
[9] D. C. Walter, B. Lim, K. Bothe, R. Falster, V. V. Voronkov, J. Schmidt, *Sol. Energy Mater. Sol. Cells* **2014**, *131*, 51.
[10] T. Niewelt, M. Selinger, N. E. Grant, W. Kwapil, J. D. Murphy, M. C. Schubert, *J. Appl. Phys.* **2017**, *121*, 185702.
[11] G. D. Watkins, *Mater. Sci. Semicond. Process.* **2000**, *3*, 227.
[12] K. J. Chang, D. J. Chadi, *Phys. Rev. B* **1989**, *40*, 11644.
[13] C. G. Van de Walle, P. J. H. Denteneer, Y. Bar-Yam, S. T. Pantelides, *Phys. Rev. B* **1989**, *39*, 10791.
[14] P. Deák, L. C. Snyder, J. W. Corbett, *Phys. Rev. B* **1988**, *37*, 6887.
[15] C. G. Van de Walle, Y. Bar-Yam, S. T. Pantelides, *Phys. Rev. Lett.* **1988**, *60*, 2761.
[16] B. Holm, K. Bonde Nielsen, B. Bech Nielsen, *Phys. Rev. Lett.* **1991**, *66*, 2360.
[17] K. Bonde Nielsen, B. B. Nielsen, J. Hansen, E. Andersen, J. U. Andersen, *Phys. Rev. B* **1999**, *60*, 1716.
[18] C. Herring, N. M. Johnson, C. G. Van de Walle, *Phys. Rev. B* **2001**, *64*, 125209.
[19] K. B. Nielsen, L. Dobaczewski, S. Søgård, B. B. Nielsen, *Phys. Rev. B* **2002**, *65*, 075205.
[20] N. M. Johnson, C. Herring, C. G. Van de Walle, *Phys. Rev. Lett.* **1994**, *73*, 130.
[21] A. Resende, R. Jones, S. Öberg, P. R. Briddon, *Phys. Rev. Lett.* **1999**, *82*, 2111.
[22] B. Bech Nielsen, K. Bonde Nielsen, J. R. Byberg, *Mater. Sci. Forum* **1993**, *143–147*, 909.
[23] M. Budde, PhD Thesis, University of Aarhus, **1998**.
[24] B. J. Hallam, P. G. Hamer, S. R. Wenham, M. D. Abbott, A. Sugianto, A. M. Wenham, C. E. Chan, G. Xu, J. Kraiem, J. Degoulange, R. Einhaus, *IEEE J. Photovoltaics* **2014**, *4*, 88.
[25] P. Hamer, B. Hallam, S. Wenham, M. Abbott, *IEEE J. Photovoltaics* **2014**, *4*, 1252.
[26] A. Van Wieringen, N. Warmoltz, *Physica* **1956**, *22*, 849.
[27] Y. V. Gorelkinskii, N. N. Nevinnyi, *Mater. Sci. Eng. B* **1996**, *36*, 133.
[28] M. Kitajima, K. Ishioka, K. G. Nakamura, N. Fukata, K. Murakami, J. Kikuchi, S. Fujimura, *Mater. Sci. Forum* **1997**, *258-263*, 203.
[29] N. Fukata, S. Sasaki, K. Murakami, K. Ishioka, K. G. Nakamura, M. Kitajima, S. Fujimura, J. Kikuchi, H. Haneda, *Phys. Rev. B* **1997**, *56*, 6642.
[30] R. E. Pritchard, M. J. Ashwin, J. H. Tucker, R. C. Newman, E. C. Lightowlers, M. J. Binns, S. A. McQuaid, R. Falster, *Phys. Rev. B* **1997**, *56*, 13118.
[31] V. P. Markevich, M. Suezawa, *J. Appl. Phys.* **1998**, *83*, 2988.
[32] R. E. Pritchard, M. J. Ashwin, J. H. Tucker, R. C. Newman, *Phys. Rev. B* **1998**, *57*, R15048.
[33] A. W. R Leitch, V. Alex, J. Weber, *Phys. Rev. Lett.* **1998**, *81*, 421.
[34] E. E. Chen, M. Stavola, W. Beall Fowler, J. A. Zhou, *Phys. Rev. Lett.* **2002**, *88*, 245503.
[35] E. E. Chen, M. Stavola, W. B. Fowler, P. Walters, *Phys. Rev. Lett.* **2002**, *88*, 105507.
[36] E. V. Lavrov, J. Weber, *Phys. Rev. Lett.* **2002**, *89*, 215501.
[37] G. A. Shi, M. Stavola, W. B. Fowler, E. E. Chen, *Phys. Rev. B* **2005**, *72*, 085207.
[38] J. W. Corbett, S. N. Sahu, T. S. Shi, L. C. Snyder, *Phys. Lett. A* **1983**, *93*, 303.
[39] A. Mainwood, A. M. Stoneham, *J. Phys. C Solid State Phys.* **1984**, *17*, 2513.
[40] S. K. Estreicher, M. A. Roberson, D. M. Maric, *Phys. Rev. B* **1994**, *50*, 17018.
[41] B. Hourahine, R. Jones, S. Öberg, R. C. Newman, P. R. Briddon, E. Roduner, *Phys. Rev. B* **1998**, *57*, R12666.
[42] S. K. Estreicher, K. Wells, P. A. Fedders, P. Ordejón, *J. Phys. Condens. Matter* **2001**, *13*, 6271.
[43] W. B. Fowler, P. Walters, M. Stavola, *Phys. Rev. B* **2002**, *66*, 075216.
[44] E. E. Chen, M. Stavola, W. B. Fowler, *Phys. Rev. B* **2002**, *65*, 245208.
[45] S. K. Estreicher, J. L. Hastings, P. A. Fedders, *Phys. Rev. B* **1998**, *57*, R12663.
[46] K. J. Chang, D. J. Chadi, *Phys. Rev. Lett.* **1989**, *62*, 937.
[47] J. D. Holbech, B. Bech Nielsen, R. Jones, P. Sitch, S. Öberg, *Phys. Rev. Lett.* **1993**, *71*, 875.
[48] C. G. Van de Walle, *Phys. Rev. B* **1994**, *49*, 4579.
[49] A. J. Tavendale, A. A. Williams, S. J. Pearton, *Appl. Phys. Lett.* **1986**, *48*, 590.
[50] E. Rimini, *Ion Implantation: Basics to Device Fabrication*. Springer US, Boston, MA **1995**.
[51] H. R. Kaufman, *J. Vac. Sci. Technol.* **1978**, *15*, 272.
[52] D. J. Sharp, J. K. G. Panitz, D. M. Mattox, *J. Vac. Sci. Technol.* **1979**, *16*, 1879.
[53] A. G. Ulyashin, R. Job, W. R. Fahrner, D. Grambole, F. Herrmann, *Solid State Phenom.* **2001**, *82-84*, 315.
[54] H. E. A Elgamel, *IEEE Trans. Electron Devices* **1998**, *45*, 2131.
[55] V. V. Voronkov, R. Falster, *Phys. Status Solidi* **2017**, *254*, 1600779.
[56] V. P. Markevich, L. I. Murin, M. Suezawa, J. L. Lindström, J. Coutinho, R. Jones, P. R. Briddon, S. Öberg, *Phys. Rev. B* **2000**, *61*, 12964.
[57] J. W. Corbett, G. D. Watkins, R. M. Chrenko, R. S. McDonald, *Phys. Rev.* **1961**, *121*, 1015.
[58] P. Johannesen, B. B. Nielsen, J. R. Byberg, *Phys. Rev. B* **2000**, *61*, 4659.
[59] J. Coutinho, R. Jones, P. R. Briddon, S. Öberg, *Phys. Rev. B* **2000**, *62*, 10824.
[60] R. K. Willardson, F. Shimura, *Semiconductors and Semimetals: Volume 42 Oxygen in Silicon*, 1st ed., Academic Press, Boston **1994**.
[61] G. D. Watkins, J. W. Corbett, R. M. Walker, *J. Appl. Phys.* **1959**, *30*, 1198.
[62] G. K. Wertheim, D. N. E. Buchanan, *J. Appl. Phys.* **1959**, *30*, 1232.
[63] J. L. Lindström, L. I Murin, V. P. Markevich, T. Hallberg, B. G. Svensson, *Phys. B Condens. Matter* **1999**, *273-274*, 291.
[64] B. Pajot, S. A. McQuaid, R. C. Newman, C. Song, R. Rahbi, *Mater. Sci. Forum* **1993**, *143–147*, 969.

[65] B. G. Svensson, J. L. Lindström, *Phys. Rev. B* **1986**, *34*, 8709.
[66] M. Mikelsen, J. H. Bleka, J. S. Christensen, E. V. Monakhov, B. G. Svensson, J. Härkönen, B. S. Avset, *Phys. Rev. B* **2007**, *75*, 155202.
[67] V. V. Voronkov, R. Falster, C. A. Londos, *J. Appl. Phys.* **2012**, *111*, 113530.
[68] V. Quemener, B. Raeissi, F. Herklotz, L. I. Murin, E. V. Monakhov, B. G. Svensson, *J. Appl. Phys.* **2015**, *118*, 135703.
[69] K. Bonde Nielsen, L. Dobaczewski, K. Goscinski, R. Bendesen, O. Andersen, B. Bech Nielsen, *Phys. B Condens. Matter* **1999**, *273–274*, 167.
[70] I. L. Kolevatov, F. Herklotz, V. Bobal, B. G. Svensson, E. V. Monakhov, *Solid State Phenom.* **2015**, *242*, 163.
[71] H. Malmbekk, L. Vines, E. V Monakhov, B. G. Svensson, *Solid State Phenom.* **2011**, *178-179*, 192.
[72] O. Feklisova, N. Yarykin, E. B. Yakimov, J. Weber, *Phys. B Condens. Matter* **2001**, *308–310*, 210.
[73] J. H. Bleka, H. Malmbekk, E. V. Monakhov, B. G. Svensson, B. S. Avset, *Phys. Rev. B* **2012**, *85*, 085210.
[74] T. L. Cottrell, *The Strengths of Chemical Bonds*. Butterworths Scientific Publications, London **1958**.
[75] B. N Mukashev, S. Z. Tokmoldin, M. F. Tamendarov, V. V. Frolov, *Phys. B Condens. Matter* **1991**, *170*, 545.
[76] V. P. Markevich, L. I. Murin, M. Suezawa, J. L. Lindström, J. Coutinho, R. Jones, P. R. Briddon, S. Öberg, *Phys. B Condens. Matter* **1999**, *273–274*, 300.
[77] G. D. Watkins, J. W. Corbett, *Phys. Rev.* **1965**, *138*, A543.
[78] P. Stallinga, P. Johannesen, S. Herstrøm, K. Bonde Nielsen, B. Bech Nielsen, J. R. Byberg, *Phys. Rev. B* **1998**, *58*, 3842.
[79] J. Coutinho, V. J. B. Torres, R. Jones, S. Öberg, P. R. Briddon, *J. Phys. Condens. Matter* **2003**, *15*, S2809.
[80] J. W. Corbett, G. D. Watkins, *Phys. Rev. Lett.* **1961**, *7*, 314.
[81] A. O. Evwaraye, E. Sun, *J. Appl. Phys.* **1976**, *47*, 3776.
[82] K. Irmscher, H. Klose, K. Maass, *J. Phys. C Solid State Phys.* **1984**, *17*, 6317.
[83] P. Lévêque, P. Pellegrino, A. Hallén, B. G. Svensson, V. Privitera, *Nucl. Instruments Methods Phys. Res. Sect. B Beam Interact. with Mater. Atoms* **2001**, *174*, 297.
[84] B. Pajot, B. Clerjaud, *Optical Absorption of Impurities and Defects in Semiconducting Crystals*. Springer, Berlin Heidelberg, Berlin, Heidelberg **2013**.
[85] Y.-H. Lee, J. W. Corbett, *Phys. Rev. B* **1976**, *13*, 2653.
[86] G. Alfieri, E. V. Monakhov, B. S. Avset, B. G. Svensson, *Phys. Rev. B* **2003**, *68*, 233202.
[87] M. Mikelsen, E. V. Monakhov, G. Alfieri, B. S. Avset, B. G. Svensson, *Phys. Rev. B* **2005**, *72*, 195207.
[88] N. Ganagona, L. Vines, E. V. Monakhov, B. G. Svensson, *J. Appl. Phys.* **2014**, *115*, 034514.
[89] P. Pellegrino, P. Lévêque, J. Lalita, a. Hallén, C. Jagadish, B. Svensson, *Phys. Rev. B* **2001**, *64*, 195211.
[90] E. V. Monakhov, A. Ulyashin, G. Alfieri, A. Y. Kuznetsov, B. S. Avset, B. G. Svensson, *Phys. Rev. B* **2004**, *69*, 153202.
[91] P. Lévêque, A. Hallén, B. G. Svensson, J. Wong-Leung, C. Jagadish, V. Privitera, *Eur. Phys. J. Appl. Phys.* **2003**, *23*, 5.
[92] B. G. Svensson, B. Mohadjeri, A. Hallén, J. H. Svensson, J. W. Corbett, *Phys. Rev. B* **1991**, *43*, 2292.
[93] I. L. Kolevatov, B. G. Svensson, E. V. Monakhov, *J. Appl. Phys.* **2018**, *124*, 085706.
[94] M. Suezawa, *Phys. Rev. B* **2000**, *63*, 035201.
[95] M. Budde, B. Bech Nielsen, J. C. Keay, L. C. Feldman, *Phys. B Condens. Matter* **1999**, *273–274*, 208.
[96] B. B. Nielsen, H. G. Grimmeiss, *Phys. Rev. B* **1989**, *40*, 12403.
[97] B. Bech Nielsen, L. Hoffmann, M. Budde, *Mater. Sci. Eng. B* **1996**, *36*, 259.
[98] J. H. Bleka, I. Pintilie, E. V. Monakhov, B. S. Avset, B. G. Svensson, *Phys. Rev. B* **2008**, *77*, 073206.